JOURNAL OF NEUROTRAUMA 36:576–588 (February 15, 2019)

DOI: 10.1089/neu.2018.5720

Chronic White Matter Degeneration, but No Tau Pathology at One-Year Post-Repetitive Mild Traumatic Brain Injury in a Tau Transgenic Model

Benoit Mouzon,[1] Corbin Bachmeier,[1] Joseph Ojo,[1] Christopher Acker,[2] Scott Ferguson,[1] Gogce Crynen,[1] Peter Davies,[2] Michael Mullan,[1] William Stewart,[3] and Fiona Crawford[1]

Abstract

Tau pathology associated with chronic traumatic encephalopathy has been documented in the brains of individuals with a history of repetitive mild traumatic brain injury (r-mTBI). At this stage, the pathobiological role of tau in r-mTBI has not been extensively explored in appropriate pre-clinical models. Here, we describe the acute and chronic behavioral and histopathological effects of single and repetitive mild TBI (five injuries given at 48 h intervals) in young adult (3 months old) hTau mice that express all six isoforms of hTau on a null murine tau background. Animals exposed to r-mTBI showed impaired visuospatial learning in the Barnes maze test that progressively worsened from two weeks to 12 months post-injury, which was also accompanied by significant deficits in visuospatial memory consolidation at 12 months post-injury. In contrast, only marginal changes were observed in visuospatial learning at six and 12 months after single mTBI. Histopathological analyses revealed that hTau mice developed axonal injury, thinning of the corpus callosum, microgliosis and astrogliosis in the white matter at acute and chronic time points after injury. Tau immunohistochemistry and enzyme-linked immunosorbent assay data suggest, however, only transient, injury-dependent increases in phosphorylated tau in the cerebral cortex beneath the impact site and in the CA1/CA3 subregion of the hippocampus after single or r-mTBI. This study implicates white matter degeneration as a prominent feature of survival from mTBI, while the role of tau pathology in the neuropathological sequelae of TBI remains elusive.

Keywords: adult head injury; age; animal studies; axonal injury; behavior

Introduction

Traumatic brain injury (TBI) has long been recognized as the strongest environmental risk factor for later development of dementia.[1,2] Although epidemiological data are strong, very little is known about the mechanistic links between exposure to a single moderate or severe TBI or repeated mild TBI (r-mTBI) and later development of neurodegenerative disease—in particular, chronic traumatic encephalopathy (CTE).[3–12] Although the polypathology of CTE is complex and multifaceted, the current preliminary pathological diagnostic criteria for CTE have been defined, with the presence of perivascular accumulation of phosphorylated tau (p-tau) in neurons and glia in a patchy distribution at the depths of cortical sulci regarded as pathognomonic.[13]

Thus far, however, no published experimental models of single or repetitive mTBI fully replicate the pathological characteristics of this neurodegenerative condition—in particular, the spectrum of tau pathologies described, including the pathognomonic lesion. Although several animal models of repetitive mTBI are described,[5,14–20] few studies report any evidence of sustained tau pathology at time points beyond the acute, post-injury period (for a review, see Ojo and associates[21]). In previous work, we have reported evidence of p-tau in two different models of r-mTBI: at 21 days after five r-mTBIs at 48 h apart in ''aged'' human tau (hTau) mice and at three months post-32 r-mTBI 72 h apart in young hTau animals.[15,22] Persistent tau pathology at six months post-injury has also been observed in wild type (WT) mice exposed to 42 r-mTBI over seven days, thus suggesting that a number of impacts may be required to trigger sustained tau pathology.[23]

Because the pathological hallmarks of Alzheimer disease (AD) including amyloid plaques and neurofibrillary tangles (NFTs) have been reported in some patients with TBI, the use of transgenic models of AD and mutated tau has also been proposed to investigate TBI pathogenesis. In this regard, Tran and colleagues[10] showed that AD (3xTg-AD) and mutated Tau (P301L) mouse models demonstrate an acute increase in tau immunoreactivity and

[1]Roskamp Institute, Sarasota, Florida.
[2]Feinstein Institute for Medical Research, Manhasset, New York.
[3]Department of Neuropathology, Laboratory Medicine Building, Queen Elizabeth University Hospital, Glasgow, Scotland.

tau phosphorylation up to two weeks after controlled cortical impact (CCI) injury. Because the cumulative effects of r-mTBI may cause the development of CTE in humans, in a recent study, Winston and coworkers[20] also explored the effects of r-mTBI in the same 3xTg-AD mice. There was no evidence of increased p-tau at either one or 30 days after repeated mild injury, however. The caveats of these models are that tau mutations are rare in the general population, tau is not present at physiological levels in mutant mice (p301L), and the models investigated thus far (e.g. WT, Tg44, p301L) do not express each hTau isoform or on a null murine background. Consequently, it is conceivable that none of these models adequately recapitulate the human tau-dependent response to TBI.

To address limitations in previous studies, in this study we address whether single or r-mTBI is associated with an acute and/or chronic p-tau pathologies in hTau transgenic animals expressing six isoforms of human, non-mutated tau on a null murine tau background,[24,25] and whether these changes correlate with altered neurobehavioral performance after injury. To this end, we will use our previously characterized closed head injury model[14,26,27] and repeat the same experimental procedures (e.g., injury paradigm, age at time of injury, interinjury interval, etc.) including behavioral, pathological, and biochemical analyses in hTau transgenic mice.

Methods

Animals

Male mice expressing hTau on a C57BL/6 and null murine tau background,[24,25] (aged 10–12 weeks, 20–24 g, Jackson Laboratories, Bar Harbor, ME) were housed singly under standard laboratory conditions (23°C ± 1°C, 50 ± 5% humidity, and 12-h light/dark cycle) with free access to food and water throughout the study. These hTau mice were generated by crossing mice that express a tau transgene derived from a human PAC, H1 haplotype, known as 8c mice,[25] with tau knockout (KO) mice in which complementary deoxyribonucleic acid (cDNA) for the enhanced green fluorescent protein (EGFP) was inserted into exon one of tau. The resulting hTau mice express all six hTau isoforms, but do not express mouse tau.[24]

Of note, the physiological tau isoform ratio (3R/4R) in the hTau mice is not 1:1 as in humans; rather, it is 4:1,[24] but still closer to mimicking physiological occurrence of hTau than WT mice or other tau transgenic models that express single isoforms of either mutated or WT tau. All procedures were performed under Institutional Animal Care and Use Committee approval and in accordance with the National Institute of Health Guide for the Care and Use of Laboratory Animals.

Injury groups and schedule

For the behavioral analyses, a total of 36 mice were assigned randomly to one of four treatment groups: single injury, single sham, repetitive injury (total of five hits with an interconcussion interval of 48 h), and repetitive sham (five anesthesias, 48 h apart). The behavior analysis began 24 h or 12 months after the sole/last mTBI/anesthesia for each group. Behavior outcomes were assessed blinded to group assignment. After the acute time point of behavioral analyses, this cohort of mice was then allowed to survive for analyses at 6 and 12 months post-injury. One animal from the r-sham group died from natural cause before the last behavioral measurement. There was no mortality rate in either mTBI group. Separately from this behavioral cohort, two other cohorts of hTau animals were assigned for pathological ($n = 20$) and biochemical ($n = 20$) examination. As before, the animals were assigned randomly to one of the four treatment groups, with five mice per group for pathology and biochemistry. All mice for pathological and biochemical analyses were euthanized at 24 h or 12 months post-sole/last mTBI/anesthesia.

Injury protocol

The mTBI was administered to mice as described previously.[14] Mice were anesthetized with 1.5 L/min of oxygen and 3% isoflurane before anesthesia or mTBI. A 5 mm blunt metal impactor tip was retracted and positioned midway relative to the sagittal suture before each impact. The injury was triggered using the myNeuroLab controller at a strike velocity of 5 m/sec, strike depth of 1.0 mm, and dwell time of 200 msec. Sham injured animals underwent the same procedures and were exposed to anesthesia for the same length of time as the mTBI animals.

Assessment of cognitive function

Learning and memory were evaluated using Barnes maze and the Ethovision XT software (Noldus) by monitoring the distance and time taken to find an escape hole over a period of six acquisition days (learning) and a final probe trial (memory). During the acquisition trials, mice were given 90 sec to locate and enter the target box. Mice were led to the target box if they did not locate it within 90 sec, and all mice were required to remain in the target box for 30 sec before retrieval, regardless of success. For a period of six days, four trials were given per day, with mice starting from one of four cardinal points on each trial. On the seventh day, a single probe trial lasting 60 sec was performed with the mouse starting from the center of the maze and the target box removed.

Assessment of anxiety

Anxiety-related and risk-taking behavior of mice were evaluated using the elevated plus maze (EPM) test, which relies on the animal's preference for dark enclosed arms rather than brightly lit, open arms at an elevated height. Time spent in the open arm is decreased in mice that exhibit anxiety-like behaviors. The maze consisted of a polyvinyl chloride plus-shaped platform elevated 50 cm from the floor with four arms intersecting at a 90-degree angle, creating four individual arms each 55 cm long and 5 cm wide. Closed and open arms were orthogonal to each other; the two closed arms were shielded by 25 cm high side and end walls, whereas the two open arms had no walls.

The experimental procedure was initiated by the placement of the mouse into the center zone (intersection point) of the maze, facing one of the open arms. The mouse was allowed to explore the maze for a 5-min period while an overhead video camera recorded the movements of each mouse. Ethovision XT was used to automatically score, in an unbiased manner, the number of entries in each of the arms as well as the time spent in each arm. All four paws of the mouse had to enter an arm for it to be considered an entry; the percentage score for the time spent in the open arm was calculated as follows: (time spent in the open arms/ [time spent in the open arms + time spent in closed arms]) × 100.

Histology

At 24 h after their last injury/anesthesia, the mice assigned to histological studies were anesthetized with isoflurane and perfused transcardially with phosphate-buffered saline (PBS), pH 7.4 followed by PBS containing 4% paraformaldehyde. After perfusion, the brains were post-fixed in a solution of 4% paraformaldehyde at 4°C for 48 h. The intact brains were then blocked and processed in paraffin using Tissue-Tek VIP (Sakura, Torrance, CA). Sagittal ($n = 5$ brains/group) and six μm sections were cut with a microtome (2030 Biocut, Reichert/Leica, Germany) and mounted on positively charged glass slides (Fisher, Superfrost Plus). Before staining, sections were deparaffinized in xylene, and rehydrated in an

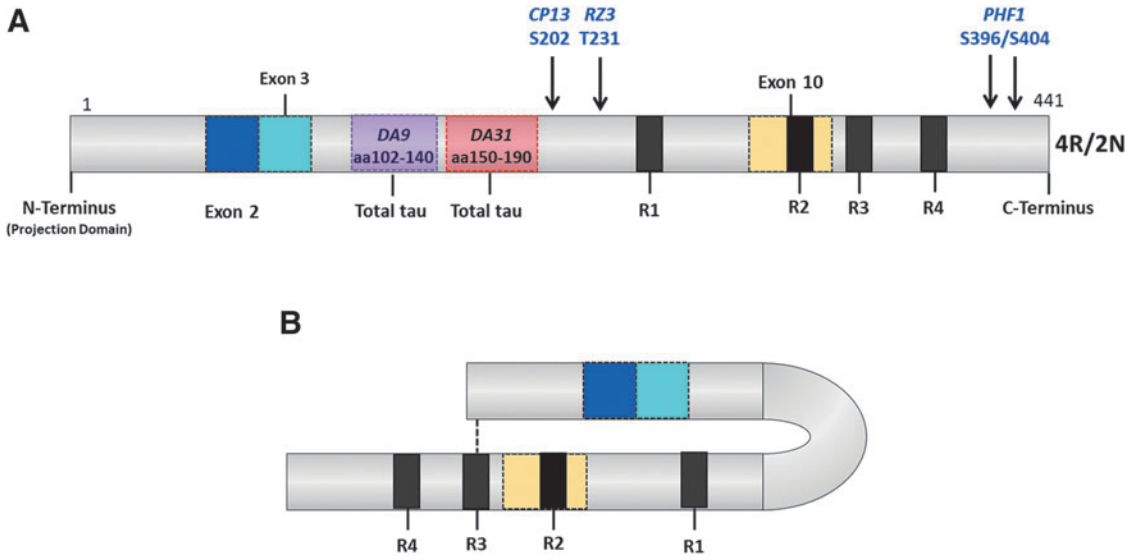

FIG. 1. Tau phosphorylation sites for the antibodies used in this study (**A**). These phosphorylation sites are found both in normal brain and Alzheimer disease brains. MC1 recognizes a very specific early pathological tau conformation produced by the intramolecular association between the extreme N-terminus (aa7–9) and the third microtubule repeat domain (aa313–322) of tau (**B**). Color image is available online at www.liebertpub.com/neu

ethanol to water gradient. For each group, sets of sagittal (lateral 0.2–0.4 mm) sections were cut. Each slide was visualized with a bright field microscope (Leica, Germany), and digital images were taken for further analysis and quantification.

Immunohistochemical quantification

For each animal, ($n = 5$ per group at 24 h and 12 months post-mTBI), sagittal sections were stained and analyzed by an observer blinded to experimental conditions using ImageJ software (US National Institutes of Health, Bethesda, MD). Using this software, images were separated into individual color channels (hematoxylin counter stain and diaminobenzidine [DAB]) using the color deconvolution algorithm. Three non-overlapping areas of 100 μm^2 for the body of the corpus callosum (CC) were selected randomly within which the area of glial fibrillary acidic protein (GFAP) immunoreactivity was calculated and expressed as a percentage of the field of view (lateral 0.2–0.4 mm). Four non-overlapping areas of 150 μm^2 between layer III and IV in the primary somatosensory cortex, and three non-overlapping areas of 100 μm^2 in the CC were selected randomly within which the area of anti-Iba1 immunoreactivity was calculated and expressed as a percentage of the field of view (lateral 0.2–0.4 mm).

The extent of axonal injury was determined in amyloid precursor protein (APP) stained sections. APP immunoreactive axonal swellings were quantified from the caudal to the dorsal area of the body of the CC. Using ImageJ software, the average thickness of the CC was calculated as described previously. A total of five slides per animal were averaged for each immunohistochemical analysis.

For tau immunohistochemistry, sections were stained with the following monoclonal antibodies at a 1:400 dilution: CP13 (pS202); PHF1 (pS396/404); RZ3 (pT231) (Fig. 1A). MC1 is a conformation-dependent antibody that reacts with both the N terminus (amino acids 7–9), and an amino acid sequence of tau in the third MTB (amino acids 313–322) that is necessary for *in vitro* formation of filamentous aggregates of tau similar to those seen in AD[28] (Fig. 1B). These Tau antibodies and protocols were generously provided by Dr. Peter Davies, The Feinstein Institute for Medical Research, Bronx, NY. A summary of antibodies used for these neuropathological analyses is shown in Table 1. Changes in CP13 and RZ3 immunoreactivity were calculated and expressed as a percentage of the field of view within the pyramidal cell layer of the CA1 and CA3 subregions of the hippocampus.

For terminal deoxynucleotidyl transferase dUTP nick end labeling (TUNEL) staining, the *in situ* cell death detection kit (Roche Diagnostics, Indianapolis, IN) was used following the manufacturer's guidelines. Labeling was performed with DAB as the chromogen. To avoid bias, positive and negative controls were included to show non-specific binding/reaction.

Table 1. Summary of Antibodies Used in This Study

Protein target	*Antibody*	*Epitope*	*IHC-Dilution*	*Source*	*Assay*
Amyloid precursor protein	22C11	Aa[a] 66–81	1:40,000	Millipore	IHC[b]
Glial fibrillary acidic protein	GFAP	GFAP	1:20,000	Dako	IHC
Anti Iba-1	Iba-1	Iba-1	1:5,000	Abcam	IHC
Amyloid beta	4G8	β-amyloid 17-2	1:500	Biolegend	IHC
Total-tau (Mouse)	DA9	aa 102–140	N/A	Dr. P. Davies	ELISA/WB[c]
Total-tau (Mouse)	DA31	aa 150–190	N/A	Dr. P. Davies	ELISA/WB[c]
Phospho-tau (Mouse)	CP13	pS202	1:400	Dr. P. Davies	ELISA/IHC/WB
Phospho-tau(Mouse)	PHF1	pS396/404	1:400	Dr. P. Davies	ELISA/IHC/WB
Phospho-tau (Mouse)	RZ3	pT231	1:400	Dr. P. Davies	ELISA/IHC/WB
Phospho-tau (Mouse)	MC1	Conformational	1:200	Dr. P. Davies	IHC

[a]aa, amino acid; [b]IHC, Immunohistochemistry; [c]ELISA, enzyme-linked immunosorbent assay.

Biochemical assessment of p-tau and total tau protein

Mice were exsanguinated via aortic puncture using a wide-bore needle to prevent hemolysis of red blood cells. Immediately after cardiac puncture, mouse brains were perfused with chilled 1X phosphate buffer saline (PBS) for 1 min to eliminate the confounding effects of blood proteins present in the brain vasculature. Brains were dissected at 4°C into hemispheres, then cortices, hippocampi, and cerebella, and then snap frozen in liquid nitrogen.

The p-tau and total tau protein were analyzed in the hemisected hippocampi and cortices obtained from all groups ($n = 5$/group). Snap-frozen hemisected cortices and hippocampi were sonicated in 0.5 mL and 0.3 mL of chilled mammalian protein extraction reagent (M-PER) buffer solution (Thermo Fisher Scientific, Waltham, MA) supplemented with protease inhibitor cocktail (Roche, Indianapolis, IN). Biochemical analyses were performed by our collaborators at the Feinstein Institute for Medical Research, Bronx, NY, to whom we sent coded tissue homogenates for quantitative assessments. Sample preparation for low-tau sandwich enzyme-linked immunosorbent assay (ELISA) and quantitation of murine-specific tau protein were performed as described previously. Total tau DA31, CP13, PHF1, and RZ3 were used as capture antibodies in the low-tau, sandwich ELISA. Data were expressed as μg tau/mg protein (tau and p-tau).

Statistics

Behavioral data were analyzed using JMP 8.0 (SAS, Cary, NC) as published previously.[14] Quantitative histologic parameters were analyzed with one-way analysis of variance (ANOVA), with a Tukey *post hoc* correction for multiple comparisons, unless indicated. ELISA data were plotted and analyzed using Graph-Pad Prism (Prism 6.01, GraphPad Software Inc. La Jolla, CA). One-way ANOVA followed by the Tukey *post hoc* test was used for comparison of soluble tau and amyloid beta 40 ($A\beta_{40}$) levels between the four groups. Only p values <0.05 were considered to be statistically significant and are indicated by an asterisk in the figures. Error bars represent the standard error of the mean (SEM).

Results

Barnes maze acquisition

To investigate whether hTau animals are more sensitive to single or r-mTBI than WT animals, we examined their learning and cognition under the same testing condition as we reported previously[14,26,27,29]: Barnes maze at two weeks, six and 12 months post-mTBI/anesthesia. Acute acquisition deficits were observed only in the repetitively injured group relative to their sham controls (Fig. 2A; r-mTBI vs. r-sham, $p < 0.05$, repeated measures ANOVA). The mean distance traveled over the six days acquisition period in the r-mTBI mice was 24% longer than that of the r-sham mice. There was no difference between the s-mTBI, s-sham, and r-sham groups at the acute time point ($p > 0.05$, repeated measures ANOVA). At chronic time-points, both injured groups traveled on average longer distances to reach the target box when compared with their respective sham groups (Fig. 2; s-mTBI vs. s-sham, $p < 0.001$; r-mTBI vs. r-sham, $p < 0.0001$ and s-mTBI vs. s-sham, $p < 0.0001$; r-mTBI vs. r-sham, $p < 0.001$, respectively, at six and 12 months after injury; repeated measures ANOVA). The average distance traveled by the s-mTBI mice over the 6-day acquisition period was 32%, and 48% longer than the s-sham mice at six and 12 months after injury, respectively. At the same time points, the r-mTBI had a greater and progressive separation on average distance traveled (62% and 28%, respectively) when compared with the r-sham. Analyses of the Barnes maze tracks on the last day of acquisition revealed that the travel path of the r-mTBI animals was more circuitous, searching in all quadrants when compared with the path of the shams of singly injured animals (data not shown).

The dataset for latency to escape was not distributed normally and thus did not satisfy the assumptions required for a repeated-measure ANOVA. The Wilcoxon signed rank test was used to test for the daily correlation between each group. No difference in escape latency performance was observed across all groups at the acute time point ($p > 0.05$) (Fig. 2). When tested at 6 and 12 months after injury, however, both injured groups showed a progressive decline in escape latency performance. At six months after injury, the mean escape latency of the s-mTBI mice improved from 87.2 sec on the first day of acquisition to 42.7 sec on their last day of acquisition. By 12 months after injury, they spent on average 89.8 sec on the first day of acquisition and 59.9 sec on their last acquisition day. In contrast, even at the six-month time point the r-mTBI mice exhibited less improvement over the six days than the other groups (see Fig. 2D; days one and six of acquisition; r-mTBI, 89.2 sec and 69.2 sec; r-sham, 83.9 sec and 42.2 sec; $p < 0.0002$); this lack of improvement during acquisition persisted at 12 months after injury (75.2 sec and 66.6 sec; $p > 0.05$). The average velocity was similar across all groups and all time points (data not shown).

Barnes maze: probe

The probe trial analyses determined the average time to reach target zone (defined by the target escape hole). At two weeks and six months post-injury, the analyses revealed that the r-mTBI mice performed the worst, followed by the r-sham, the s-mTBI, and the s-sham (Fig. 3). While there was a trend for both injured groups to perform worse than their respective sham groups, the time to reach the target or adjacent holes did not reach statistical significance ($p > 0.05$ for both injury groups; ANOVA). Probe test performance was only markedly impaired in the r-mTBI mice compared with both control groups at 12 months post-injury, requiring on average 32 sec to reach the target zone, as determined by one-way ANOVA followed by Tukey *post hoc* test ($p > 0.05$). The mean velocity for the probe trial was similar across all groups ($p > 0.05$).

Elevated plus maze

To characterize the long-term effects of single or repetitive mild TBI on anxiety-related behaviors, the exploratory activity of each animal was tested in the elevated-plus maze (Supplementary Fig. 1; see online supplementary material at http://www.liebertpub.com). There was no difference in the percentage of time spent in the open arms across all groups. (s-sham, $32.72 \pm 13.17\%$; r-sham, $39.77 \pm 12.12\%$; s-mTBI, $36.19 \pm 11.76\%$; r-mTBI, $48.15 \pm 12.12\%$; $p > 0.05$ one-way ANOVA followed by the Tukey *post hoc* test).

Macroscopic pathology

Consistent with previous experience, there were no skull fractures, cerebral hemorrhages, or contusions identified using this injury model in hTau mice, save for evidence of focal microhemorrhage (<1 mm^2) in the inferior surface of the cerebellum in all animals that underwent r-mTBI. Otherwise, the brains of the hTau animals had no gross macroscopic differences when compared with the WT animals.

GFAP immunostaining

To determine whether a similar astroglial response occurs in the brains of the hTau animals as we observed in the brain of the WT mice,[14,26,27,30] histological analyses were performed in the brain

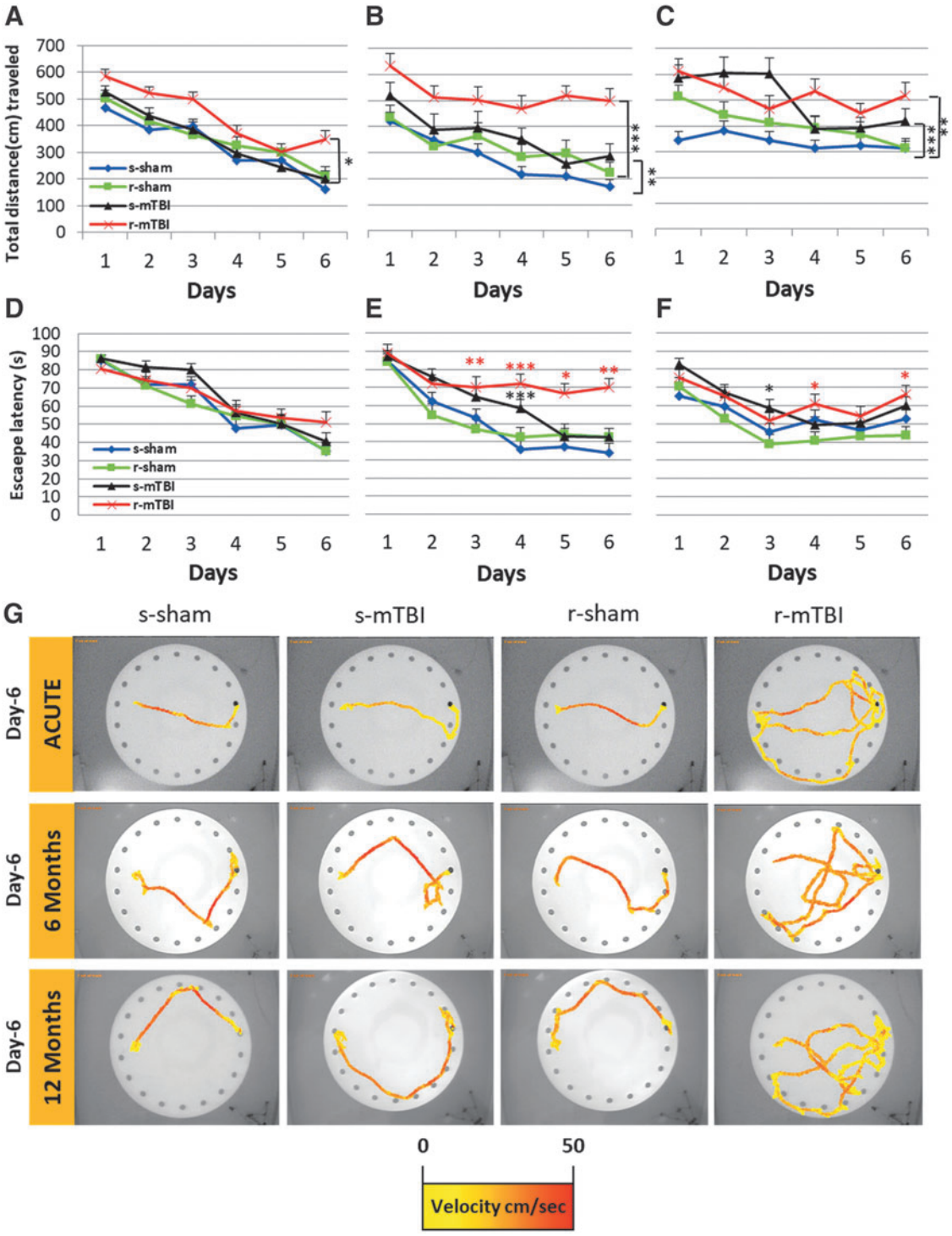

FIG. 2. Evaluation of learning (acquisition) using the Barnes maze at 14 days, six and 12 months post mild traumatic brain injury (mTBI). Mice were tested in the Barnes maze for their ability to locate a black box at the target hole. (**A**) During the acquisition testing at an acute time point post-injury, all mice had similar learning rate. The repetitive mTBI (r-mTBI) group, however, traveled a greater distance before escaping to the target hole when compared with their respective anesthesia controls (r-sham vs. r-mTBI $*p < 0.05$; repeated-measures analysis of variance [ANOVA]). (**B**) By six months post-injury, both injured group had a longer traveling path before escaping the maze (s-sham vs. s-mTBI $**p < 0.001$; r-sham vs. r-mTBI $***p < 0.0001$; repeated-measures ANOVA). At this same time point, the learning rate of the r-mTBI group was impaired when compared with the three other groups. (**C**) By 12 months post, all groups traveled a longer distance before escaping the maze with both injured groups performing worse than their sham counterparts (s-sham vs. s-mTBI $***p < 0.0001$; r-sham vs. r-mTBI $**p < 0.001$; repeated-measures ANOVA). (**D**) At acute time point post-injury, there was no difference in the escape latency across each group. (**E,F**) On day 3, 4, 5, and 6 of the acquisition trial at six months post-injury and on days 4 and 6 at 12 months post-injury, the r-mTBI group spent a longer length of time to find the escape target hole when compared to the r-sham (red asterisks; Wilcoxon signed rank test, $*p < 0.05$, $**p < 0.01$, $***p < 0.0001$). (E,F) The s-mTBI group spend a longer length of time to escape the maze on day 4 and day 3 at six and 12 months post mTBI, respectively (black asterisks; Wilcoxon signed rank test, $*p < 0.05$, $***\mathbf{p} < 0.0001$). Data are presented as mean ± standard error of the mean; $n = 9$ per group. (**G**) Traces of Barnes maze performance from each animal in each group during the last day of acquisition starting on the west side of the table. The gradient color line indicates the velocity (cm/sec) of the tested animal. Color image is available online at www.liebertpub.com/neu

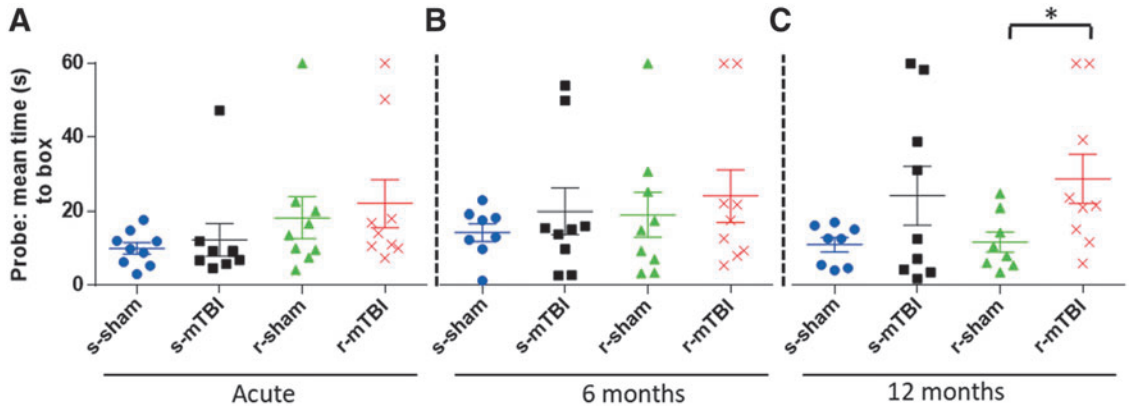

FIG. 3. Evaluation of spatial memory retention (probe) using the Barnes maze at 12 weeks, six and 12 months post mild traumatic brain injury (mTBI). For the probe trial (1 day after the six days of acquisition testing), the target box was removed and mice were placed in the middle of the table for a single, 60-sec trial. Probe test performance was not impaired at acute or six months post mTBI. At 12 months post mTBI, spatial learning was markedly impaired in the repetitive mTBI (r-mTBI) group $*p<0.05$ at 12 months as determined by the Student *t* test). Data are presented as mean ± standard error of the mean; $n=9$ per group at acute time point, $n=8$ for the s-sham at six months post-injury and $n=8$ for s-sham and r-sham at 12 months post-injury. Color image is available online at www.liebertpub.com/neu

regions known to be affected in this model of mTBI. For all groups, the cortical region underlying the impact site (somatosensory and primary motor cortices), the CC, and the hippocampal regions were assessed in sections stained for GFAP. No astrocytes with morphological appearances of reactive glia, manifest as GFAP immunoreactive astrocytes with thickened cell processes and hypertrophied cell soma, were observed in the cortex or in hippocampal sector CA1 (data not shown) at 24 h or 12 months after single or repetitive anesthesia shams.

Regarding the CC, the r-mTBI group showed an increased GFAP immunoreactivity at both 24 h and 12 months post-injury (significant main effect of treatment by ANOVA $F[3, 32]=10.63$ $p<0.0001$; *post hoc* comparison shows difference between r-mTBI 11.2 ± 2.5% vs. r-sham 2.3 ± 0.4% at 24 h post-injury and a significant main effect of treatment by ANOVA $F[3, 74]=8.369$ $p<0.0001$; *post hoc* comparison shows difference between r-mTBI 10.9 ± 1.1% vs. r-sham 4.8 ± 0.5%; $p<0.05$ at 12 months post-injury; $p<0.05$; Fig. 4,5). Notably, although there was no measurable increased GFAP immunoreactivity in the CC at 24 h post-injury when compared with their corresponding sham, there was a mild increase in immunoreactivity at 12 months post-injury (s-mTBI 3.0 ± 0.9% vs. s-sham 3.6% ± 0.45% at 24 h post-injury and s-mTBI 7.2 ± 1.1% vs. s-sham 4.6 ± 1.0%; $p<0.05$ at 12 months post-injury; $p<0.05$; Fig. 4,5). In the region of the cortex underlying the impact site, a mild reactive astrogliosis was only observed at 24 h post-injury in the r-mTBI (data not shown). In the CA1 region, there was no evidence of increased immunoreactivity within the injured groups (data not shown).

APP immunostaining

Numerous APP-immunoreactive axonal profiles were identified in sections from both injury groups (Fig. 4,5). These APP-immunoreactive axonal profiles were observed as either granular or more elongated, fusiform swellings in the white matter of the parasagittal cortex, including the splenium, body, and genu of the CC, and the spinal trigeminal tracts of the brainstem (BS). APP-immunoreactive axonal profiles were observed at 24 h and 12 months post-injury in the CC of the s-mTBI (Fig. 4,5F) and r-mTBI groups (Fig. 4,5H) but not in their controls (Fig. 4,5E,G). The numbers of APP-immunoreactive profiles in the CC of the s-mTBI was greater than in the r-mTBI group at 24 h post-injury (s-mTBI group 18 ± 2.26 vs. r-mTBI 14 ± 0.8 axonal profiles/100 μm^2; $p<0.001$), contrasting with higher numbers of positive profiles in the r-mTBI when compared with s-mTBI at 12 months (s-mTBI group 3.4 ± 0.9 vs. r-mTBI 11.5 ± 1.4 axonal profiles/100 μm^2 $p<0.001$) (Fig. 4,5). At 24 h post-injury, axonal damage in the BS was minimal in the s-mTBI, whereas greater numbers of punctate immunoreactive swellings were present in the r-mTBI group. There was no evidence of ongoing axonal injury in the BS at 12 months post-injury.

Ionized calcium binding adaptor molecule 1 immunostaining

No evidence of ongoing, active neuroinflammation was identified in sections stained for ionized calcium binding adaptor molecule 1 (Iba1) in the hTau sham animals at any time point (Fig. 4,5). In the single injury animals, both resting and activated microglia (with a bushy morphology) were observed at 24 h post-injury in the CC (significant main effect of treatment by ANOVA $F[3, 68]=79.84$ $p<0.0001$; and *post hoc* comparisons show difference between s-mTBI 6.22 ± 0.9% vs. s-sham 3.22 ± 0.9%; $p<0.05$; Supplementary Fig. 2; see online supplementary material at http://www.liebertpub.com) and in the cortex (Fig. 4J) (significant main effect of treatment by ANOVA $F[3, 68]=60.58$ $p<0.0001$; and *post hoc* comparisons show difference between s-mTBI 6.2 ± 0.9% vs. s-sham 4.01 ± 0.3%; $p<0.001$; Fig. 4J).

For mice that underwent r-mTBI, immunostaining for Iba1 revealed clusters of activated microglia in the CC (significant main effect of treatment by ANOVA $F[3, 68]=79.84$ $p<0.0001$; and *post hoc* comparisons show difference between r-mTBI 13.7 ± 1.3% vs. r-sham 2.21 ± 0.6%; $p<0.0001$; s-mTBI 6.22 ± 0.9% vs. r-mTBI 13.7 ± 1.3%; $p<0.05$; Supplementary Fig. 2; see online supplementary material at http://www.liebertpub.com), and microglia with a bushy morphology in the region of the cortex underlying the impact site (significant main effect of treatment by ANOVA $F(3, 68)=60.58$ $p<0.0001$; and *post hoc* comparisons show difference between r-mTBI 10.4 ± 1.3% vs. r-sham 2.01 ± 0.5%; $p<0.0001$; s-mTBI 6.2 ± 0.9% vs. r-mTBI 10.4 ± 1.3%; $p<0.05$; Fig. 4L). By 12 months post-injury, there was no evidence of activated microglia in the cortical region of any groups. For the single and r-mTBI, however,

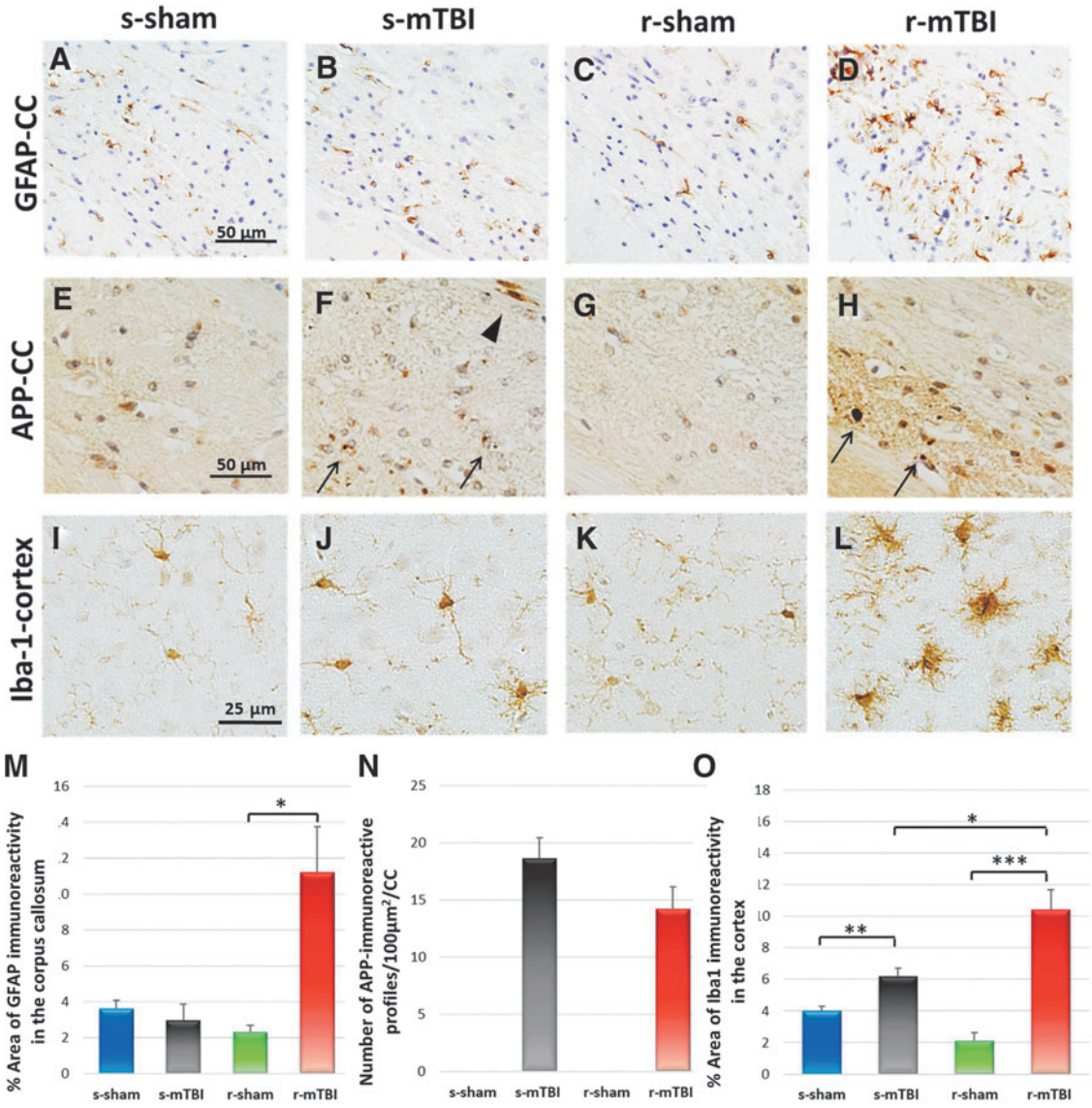

FIG. 4. Neuropathological features at 24 h after sole/last mild traumatic brain injury (mTBI) of sagittal sections of mouse brain at ≈0.4 mm lateral to the midline. Glial fibrillary acidic protein (GFAP) immunohistochemistry in the corpus callosum (**A–D**). There were no changes in the s-mTBI group (B) compared with their respective sham group (A). An increase in the area of GFAP staining was observed in the repetitive mTBI (r-mTBI) at 24 h after final injury in the corpus callossum (D). Quantitative analysis of GFAP staining in three 100 μm2 areas of the splenium of the corpus callosum at 24 h post last mTBI (r-sham 2.3 ± 0.4% vs. r-mTBI 11.2 ± 2.5%; $p < 0.05$) (**M**). Immunoreactive axonal profiles were observed in the corpus callosum as either granular (arrow) or more elongated, fusiform (arrow head) swellings in both s-mTBI (**F**) and r-mTBI groups (**H**). Tissue staining from s-sham (**E**), and r-sham animals (**G**) was negative for amyloid precursor protein (APP) immunostaining. Average counts of APP-immunoreactive axonal profiles per 100 μm^2 in the corpus callosum (s-mTBI group 18.5 ± 1.8 vs. r-mTBI 14.1 ± 1.9 axonal profiles/ 100 μm^2 of corpus callosum (**N**). Immunohistochemical labeling for microglia with anti-Iba1. There was no microglial activation in the sham (**I**) and r-sham (**K**) groups. A mild increased area of Iba1 immunoreactivity with few cells having a bushy morphology was observed in the region of the cortex underlying the impact site at 24 h post s-mTBI (**J**). For mice that underwent r-mTBI, immunostaining for anti-Iba1 revealed clusters of activated microglias with hypertrophic and bushy morphology in the region of the cortex underlying the impact site (**L**). Quantitative analysis of Iba1 staining in three 200 μm^2 fields between layer III and V of the cortex at 24 h post-sole/last mTBI (**O**). Tissue sections were counter-stained with hematoxylin. $n = 5$/group, respectively. Data are presented as mean ± standard error of the mean, (*$p < 0.05$; **$p < 0.005$; ***$p < 0.0005$). Color image is available online at www.liebertpub.com/neu

increased microglial activity in the splenium and body of the CC was observed when compared with corresponding shams (r-mTBI 10.4 ± 1.3% vs. r-sham 3.01 ± 0.5%; $p < 0.0001$; s-mTBI 6.1 ± 0.9% vs. s-sham 3.4 ± 0.7%; $p < 0.05$; Supplementary Fig. 2; see online supplementary material at http://www.liebertpub.com).

Tau immunohistochemistry in the cortex

No TBI-dependent increase in cortical soluble p-tau CP13 (Fig. 6A–C), RZ3 (Fig. 6D–F) or PHF1 (Fig. 6G-I) was observed at 24 h or 12 months post-injury measured by ELISA analyses ($p > 0.05$;

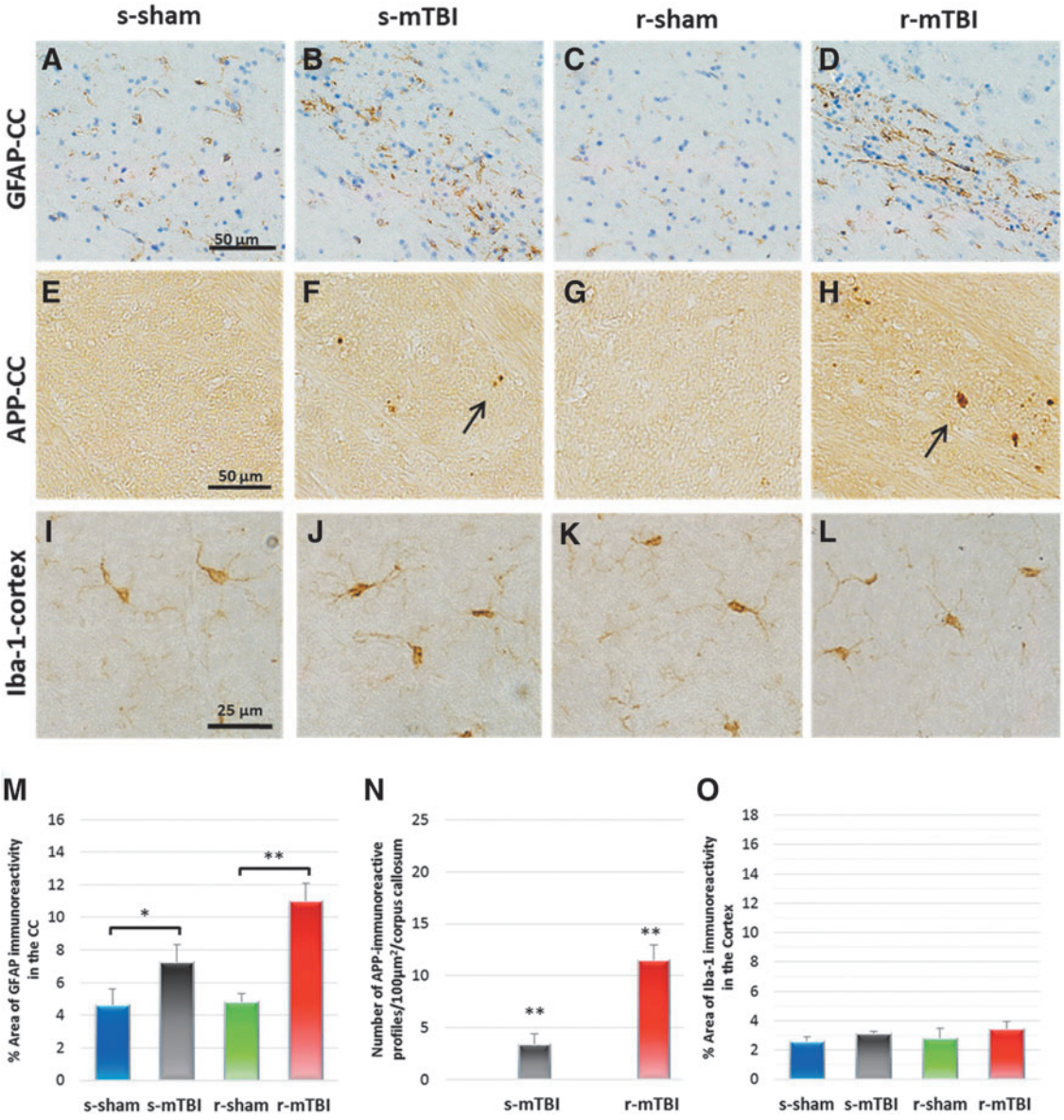

FIG. 5. Neuropathological features at 12 months after sole/last mTBI of sagittal sections of mouse brain at ≈0.4 mm lateral to the midline. Glial fibrillary acidic protein (GFAP) immunohistochemistry in the corpus callosum (CC) (**A–D**). Healthy astrocytes with quiescent morphology were observed in sham animals at both time points. At 12 months after injury, the single mTBI (s-mTBI) animals exhibited mild reactive astrogliosis with variable degrees of thickened cell processes and hypertrophic cell soma (s-mTBI 7.2 ± 1.1% vs. s-sham 4.6 ± 1.0%; $p < 0.05$ at 12 months post injury; $p < 0.05$; A,B,**M**). Severe reactive astrogliosis was also observed in the repetitive mTBI (r-mTBI) group as early as 12 months post-injury (r-mTBI 10.9 ± 1.1% vs. r-sham 4.8 ± 0.5%; $p < 0.05$ at 12 months post injury; $p < 0.05$; Fig. 6 C,D,M). Granular axonal profiles stained positively with the axonal injury marker amyloid precursor protein (APP) were seen predominantly after single r-mTBI within the CC when compared with their control groups. (**F**) The density of APP-immunoreactive profiles per unit area in the body of the CC of the r-mTBI group was greater than in the s-mTBI group at 12 months after mTBI (s-mTBI group, 3.4 ± 0.9 vs. r-mTBI 11.5 ± 1.4 axonal profiles/body of CC, $p < 0.001$; Fig. 6 F,H,N). For all groups, there was no appreciable evidence of microglial activation in motor cortex at 12 months post-injury ($p > 0.05$; Fig. 6 I). Color image is available online at www.liebertpub.com/neu

one-way ANOVA). Nonetheless, an age-dependent increase for each soluble p-tau CP13 and RZ3 immunoreactivity was observed between 24 h and 12 months post-mTBI in the cortices of all groups ($p < 0.01$; one-way ANOVA followed by Tukey *post hoc t* test). In animals that underwent single and repetitive mTBI, however, an increase of CP13, RZ3 and PHF1 immunoreactivity was observed in cell bodies and apical dendrites of occasional cortical neurons underlying the impact site at 24 h post-injury, while no cortical neurons were labeled in control groups (Fig. 6C,F,I). These p-tau neurons was not persistent at the chronic time point of 12 months after injury. There was no increase of p-tau when quantitated as a ratio of p-tau protein to total tau protein with ELISA (Fig. 6B,E,H).

Tau immunohistochemistry in the hippocampus

The low-tau ELISAs that quantitatively assess different epitopes of tau did not reveal any TBI-dependent increase in cortical soluble p-tau CP13 (Fig. 7A-C), RZ3 (Fig. 7D-F) and PHF1 (Fig. 7G-I)

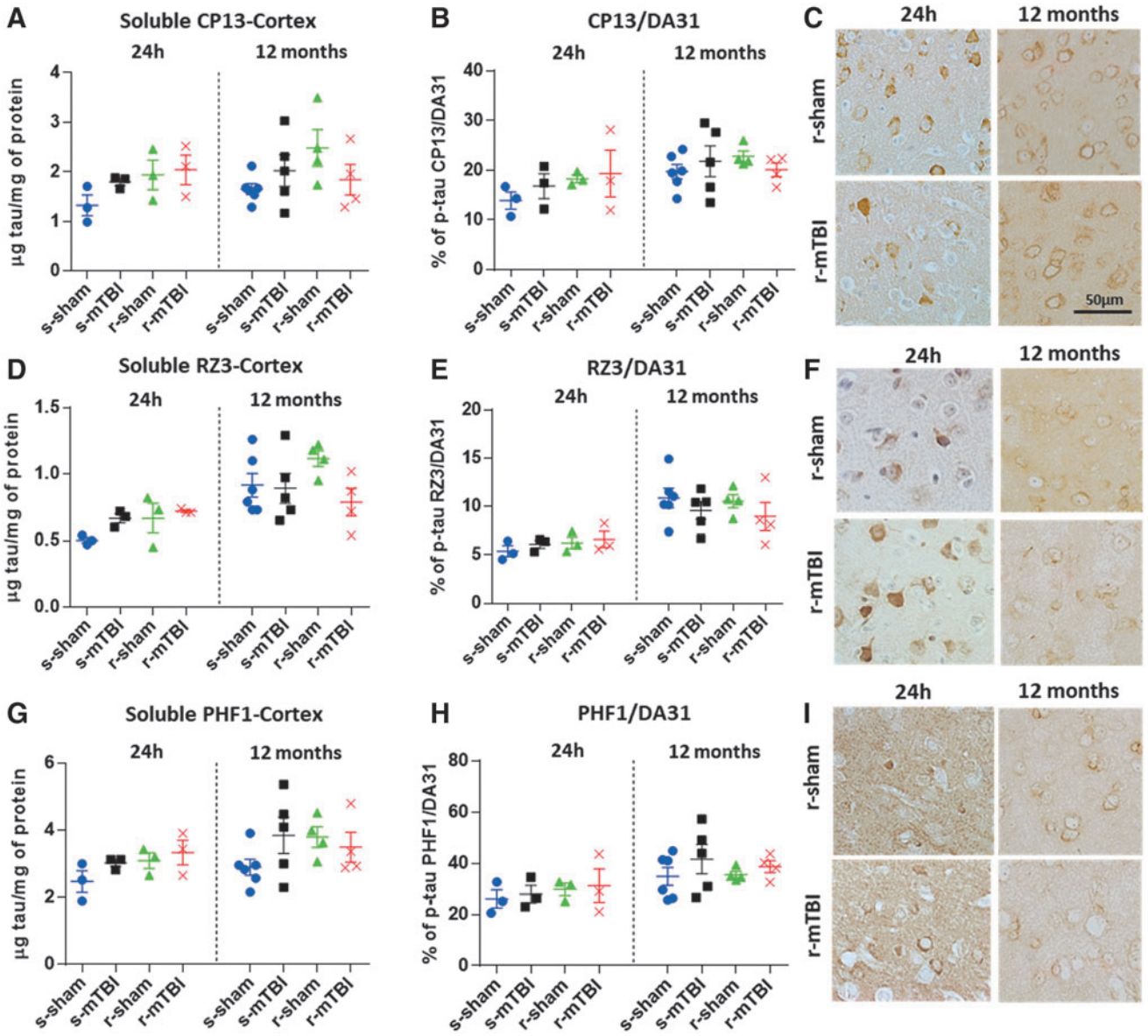

FIG. 6. Biochemical (enzyme-linked immunosorbent assay) and immunohistochemical assessment of different soluble phosphorylated tau (p-tau) species in the neocortex at 24 h and 12 months after injury. (**A,D,G**) There was no traumatic brain injury (TBI)-dependent increase in cortical soluble p-tau pSer-202 (CP13), pThr-231 (RZ3), and pSer-396/404 (PHF1) at 24 h or 12 months after mild TBI (mTBI) ($p > 0.05$; one-way analysis of variance [ANOVA]). An age-dependent increase for each soluble p-tau was observed between 24 h and 12 months after mTBI in the cortices of all groups ($p < 0.0001$; one-way ANOVA followed by Tukey *post hoc t* test). (**B,E,H**) Each data point indicates an individual animal. Similar to the quantitative analysis of each p-tau epitope, there was no increase of p-tau when quantitated as a ratio of p-tau protein to total tau protein. (**C,F,I**) p-Tau immunohistochemistry of mouse brain at approximately 0.5 mm lateral to midline in the superficial layers of the cerebral cortex. (C,F) All experimental groups exhibited somatodendritic localized accumulation of CP13 and RZ3 immunoreactivity in neurons of the superficial layer of the cerebral cortex. (I) No PHF1 immunoreactivity was observed in injured or sham animals at 24 h and 12 months after injury. Qualitative assessment of tau immunohistochemistry revealed no change between sham and injured animals at six and 12 months after injury in all groups. Color image is available online at www.liebertpub.com/neu

at 24 h and 12 months post-injury ($p > 0.05$; one-way ANOVA). Qualitative observation of the IHC-stained sections, however, revealed a trend for increased immunostaining for CP13 and RZ3 within the CA1 and CA3 subregion of the hippocampus in both injured groups when compared with their respective shams at 24 h post-injury. Generally, the r-mTBI group showed greater dendritic and membranous staining than the other groups. In addition, p-tau was also quantitated as a ratio of p-tau protein to total tau protein. No change was observed, however, for p-tau CP13, RZ3, and PHF1 in sham and injured animals (Fig. 7B,E,H).

Soluble DA31 (total tau) ELISA and aggregated tau MonoELISA DA9-DA9HRP

In all experimental groups, at both 24 h and 12 months after mTBI/anesthesia, there was no TBI-dependent increase in cortical

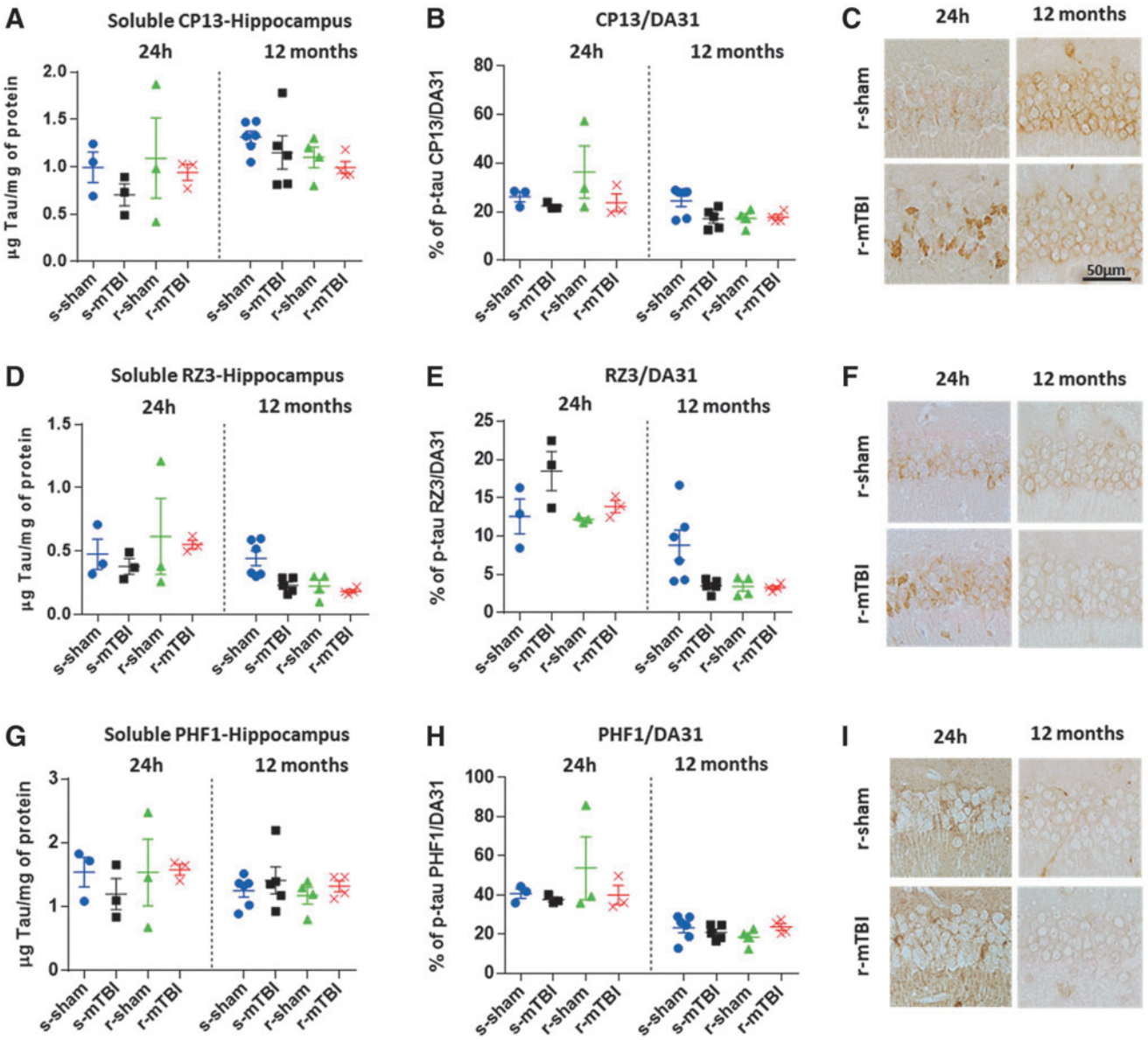

FIG. 7. Biochemical (enzyme-linked immunosorbent assay) and immunohistochemical assessment of different soluble phosphorylated tau (p-tau) species in the hippocampus at 24 h and 12 months after injury. (**A,D,G**) There was no traumatic brain injury (TBI)-dependent increase in hippocampal soluble p-tau pSer-202 (CP13), pThr-231 (RZ3), and pSer-396/404 (PHF1) at 24 h or 12 months after mild TBI (mTBI) ($p > 0.05$; one-way analysis of variance [ANOVA]). Each data point indicates an individual animal. (**B,E,H**) Similar to the quantitative analysis of each individual p-tau epitope, there was no increase in p-tau when quantitated as a ratio of p-tau protein to total tau protein. (**C,F,I**) p-Tau immunohistochemistry of mouse brain at approximately 0.5 mm lateral to midline in the CA1 region of the hippocampus. All experimental groups exhibited somatodendritic accumulation of CP13 and RZ3 immunoreactivity in the pyramidal cell layer of the hippocampus. There was no change between sham and injured animals at 24 h and 12 months after injury in all groups. Color image is available online at www.liebertpub.com/neu

or hippocampal soluble tau (Supplementary Fig. 3; see online supplementary material at http://www.liebertpub.com; $p > 0.05$) and aggregated tau (Supplementary Fig. 4; see online supplementary material at http://www.liebertpub.com; $p > 0.05$). An age-dependent increase in aggregated tau was observed between 24 h and 12 months post-in the cortex (Supplementary Fig. 4; $p < 0.001$).

Amyloid biochemistry/immunohistochemistry

No evidence of amyloid pathology was identified in r-mTBI injured animals (diffuse or neuritic Aβ plaques), as determined by histopathology in sections from cortex or hippocampus stained for 4G8 or Congo red at 24 h or 12 months after mTBI/anesthesia (data not shown). Further, ELISA analysis of soluble murine Aβ40 showed no TBI or age-dependent increases (data not shown).

TUNEL

Pyramidal neurons of the hippocampus and neurons that stained positive for Tau in the cortex were devoid of TUNEL positive staining, indicating that there was no apoptotic programmed cell death in either sham or injured animals (data not shown).

Discussion

Here we report observations on acute and chronic effects of single and r-mTBI in a transgenic mouse model to explore the potential role of tau pathobiology after mTBI. Our data show that single and r-mTBI induced a modest increase in the cortical soluble fraction of three different p-tau epitopes: CP13, PHF1, and RZ3 that resorbed by 12 months post-injury. This increase was not associated with worse behavioral performance when compared with our previous reports in WT animals with the same experimental design.[14,26,27] In addition, we showed that the post-TBI neuropathology in hTau and WT mice was otherwise comparable, with essentially similar levels of axonal injury and chronic neuroinflammation in both study groups.

Very little is known about the mechanisms involved in the accumulation of tau proteins observed in human cases late after mTBI. Evidence from a pre-clinical model of TBI demonstrates rapid formation of neurotoxic oligomeric and p-tau aggregates that may be followed by a toxic gain of function.[31] Therefore, we questioned whether r-mTBI could increase soluble p-tau in our model at 24 h post-injury and whether these changes were transient or sustained, possibly leading to pre-tangle formation. Our data confirm an increase in CP13 (pS202) and RZ3 (pT231) acutely post-injury; however, this change was transient. Further work is required to address the time course and the presence, if any, of other tau species such as soluble small oligomers, and insoluble tau species. The absence of aggregated tau and MC1 immunostaining suggests, however, that our injury paradigm does not trigger the formation of toxic tau conformational species at 24 h and 12 months post-single and r-mTBI.

Our immunohistochemical observations showed an increase in somatodendritic p-tau (CP13, PHF1, RZ3) in the superficial layer of the cortex at 24 h, but not at 12 months, in injured animals. Supporting these observations, ELISA of the cortical homogenate also revealed a trend toward an elevation of p-tau epitopes pS202 and pT231 at 24 h but not at 12 months post-injury. In the hippocampus, despite subtle changes in p-tau levels as determined by ELISA, we observed a dramatic increase in p-tau immunoreactivity to the pyramidal layer of the hippocampus, but again these changes were transient in nature suggesting that our rodent injury paradigm does not replicate the pathology that has been described many years after r-mTBI in human CTE cases.

In our model, we used hTau mice that express all six hTau isoforms on a null murine background. Unlike humans that express 3R:4R tau isoform ratio at (50:50), however, they have been reported to express a higher 3R:4R tau isoform ratio (4:1).[24] Changes in the tau isoform ratio are associated with distinct tauopathies—for example, a shift toward an increase of 4R isoforms is observed in patients with progressive supranuclear palsy or argyrophilic grain disease, whereas a shift toward an increase of 3R is associated with frontotemporal dementia with parkinsonism-17 (FTDP17).[32]

The effects of some of the FTDP-causing mutations in tau (for example; P310L, V337M and G272V) have been extensively studied in transgenic mice that develop widespread NFTs,[33,34] and these studies as well as *in vitro* cell culture models suggest that the 4R tau isoform is potentially a more favorable substrate for aberrant hyperphosphorylation and also has the propensity to self-aggregate into filaments more readily at a lower phosphorylation stoichiometry.[35] Therefore, the significant imbalance in the 3R:4R tau ratio in our hTau mouse model may be an important factor in the appearance of tau pathology after injury and should be considered in the interpretation of our data.

Based on these results, it remains unclear whether the acute increase of cortical tau phosphorylation originates from the endogenous pool of tau from formerly healthy axons damaged by injury or from tau newly synthesized as a response to cytoskeletal damage. While further work is required to answer this question, TUNEL staining revealed no apoptotic neurons in the cortex or hippocampal regions in sham or injured animals. This suggests that neurons showing enhanced somatodendritic phosphorylated tau staining are not apoptotic. Owing to its known involvement in AD pathogenesis, tau has been considered in general as a disease-causing agent. The potential link between a transient surge of tau hyperphosphorylation, however, as observed after TBI, and neurodegeneration has not yet been clearly defined. In fact, evidence suggests that tau phosphorylation at certain sites (e.g., KXGS motifs) may protect against tau aggregation.[36] In addition, Arendt and colleagues[37] revealed that hyperphosphorylation of tau in hibernating animals reverses rapidly on arousal from torpor. Similar to these observations from hibernating animals, tau hyperphosphorylation resulting from TBI might potentially involve an intrinsic response to protect the neurons from further damage through mechanisms that stabilize the cytoskeleton and synaptic structure.[38,39]

Other pathological features seen in human CTE cases, such as perivascular tau pathology, neuropil threads, and astrocytic tangles,[6] were not observed in our mouse model of mTBI. It is possible that these differences between human CTE cases and our mouse model may be constrained by differences in the severity and frequency of injury, interspecies differences; including the rodent inherent ability in clearing hyperphosphorylated tau, the craniospinal angle, the significantly greater deformability of the murine skull, and the white to gray matter ratio in mice and humans. Overall, these data seem to suggest that tau hyperphosphorylation at acute time points post-injury may be a normal physiological response of the brain after mTBI.

Our findings also raise the question concerning the link between anesthesia exposure and increased tau phosphorylation, which have been reported on several occasions in the literature.[40–42] Indeed, a trend for lower spatial memory performance (Barnes maze probe trial) was observed in the r-sham group. The pathological examination also revealed a tendency for increased tau phosphorylation in mice with multiple anesthesia exposures. This trend was not observed in our previous study in aged hTau mice.[22] This could be explained by the transient increase of tau phosphorylation that resorbs within weeks post-exposure[43] or by the fact that aged tau mice have such high levels of p-tau that they supersede that which could be induced by anesthesia.

When tested for behavioral performance in the Barnes maze, the r-mTBI group showed impaired learning consistent with our mTBI study in WT mice at both time points tested (24 h and 12 months post-injury).[26] In contrast to our previous study, however, the single injury paradigm failed to demonstrate any significant effect on the behavior of the hTau mice because they performed at the same level as their sham control counterparts at the acute time point (in terms of escape latency and distance traveled).

Alterations in genetic background of the animals could be the cause of such differences, because mice that have been manipulated genetically are known to perform differently in certain behavioral tests. It is interesting to note that the overall performance of the young hTau mice was superior to the young WT groups because they were able to find the hidden box with the shortest distance and time traveled when compared with WT animals over the acquisition trial phase, although they performed worse on the probe trial at both time points. We did not observe an increase in the time spent in the open arms of the maze at the chronic time point, suggesting that the mice do not express risk-taking behavior at this stage.

To date, many reports on human pathology in CTE have consistently focused on the development of p-tau pathology years after exposure to TBI.[6,44,45] The majority of these studies, however, have been retrospective in nature and from convenience samples of clinically symptomatic cases with inherent biases in case selection. The experimental data presented here and in previous pre-clinical models continue to suggest neuroinflammation and axonal injury, rather than tau pathology, have a significant role in the neuropathological events after single or repetitive mTBI; these pathologies in turn show strong correlation with the acute and chronic behavioral changes observed post-injury.

Acknowledgment

This research was funded by a Department of Defense award (W81XWH-10-1-0759) to Dr. Fiona Crawford, and by the Roskamp Foundation. Dr. Crawford is a VA Research Career Scientist. Dr. Stewart is supported by NIH grants R01NS038104 & R01NS094, DOD and an NHS Research Scotland Career Research Fellowship. Any opinions, findings, conclusions or recommendations expressed in this publication are those of the author(s) and do not necessarily reflect the views of the U.S. Government, or the U.S. Department of Veterans Affairs, and no official endorsement should be inferred.'

Author Disclosure Statement

No competing financial interests exist.

References

1. Lehman, E.J., Hein, M.J., Baron, S.L., and Gersic, C.M. (2012). Neurodegenerative causes of death among retired National Football League players. Neurology 79, 1970–1974.
2. Plassman, B.L., Havlik, R.J., Steffens, D.C., Helms, M.J., Newman, T.N., Drosdick, D., Phillips, C., Gau, B.A., Welsh-Bohmer, K.A., Burke, J.R., Guralnik, J.M., and Breitner, J.C. (2000). Documented head injury in early adulthood and risk of Alzheimer's disease and other dementias. Neurology 55, 1158–1166.
3. Johnson, V.E., Stewart, W., and Smith, D.H. (2010). Traumatic brain injury and amyloid-beta pathology: a link to Alzheimer's disease? Nat. Rev. Neurosci. 11, 361–370.
4. Johnson, V.E., Stewart, W., and Smith, D.H. (2012). Widespread tau and amyloid-beta pathology many years after a single traumatic brain injury in humans. Brain Pathol. 22, 142–149.
5. Mannix, R., Meehan, W.P., Mandeville, J., Grant, P.E., Gray, T., Berglass, J., Zhang, J., Bryant, J., Rezaie, S., Chung, J.Y., Peters, N.V., Lee, C., Tien, L.W., Kaplan, D.L., Feany, M., and Whalen, M. (2013). Clinical correlates in an experimental model of repetitive mild brain injury. Ann. Neurol. 74, 65–75.
6. McKee, A.C., Stern, R.A., Nowinski, C.J., Stein, T.D., Alvarez, V.E., Daneshvar, D.H., Lee, H.S., Wojtowicz, S.M., Hall, G., Baugh, C.M., Riley, D.O., Kubilus, C.A., Cormier, K.A., Jacobs, M.A., Martin, B.R., Abraham, C.R., Ikezu, T., Reichard, R.R., Wolozin, B.L., Budson, A.E., Goldstein, L.E., Kowall, N.W. and Cantu, R.C. (2013). The spectrum of disease in chronic traumatic encephalopathy. Brain 136, 43–64.
7. Smith, C., Graham, D.I., Murray, L.S., and Nicoll, J.A. (2003). Tau immunohistochemistry in acute brain injury. Neuropathol. Appl. Neurobiol. 29, 496–502.
8. Smith, D.H., Johnson, V.E., and Stewart, W. (2013). Chronic neuropathologies of single and repetitive TBI: substrates of dementia? Nat. Rev. Neurol. 9, 211–221.
9. Tran, H.T., LaFerla, F.M., Holtzman, D.M., and Brody, D.L. (2011). Controlled cortical impact traumatic brain injury in 3xTg-AD mice causes acute intra-axonal amyloid-beta accumulation and independently accelerates the development of tau abnormalities. J. Neurosci. 31, 9513–9525.
10. Tran, H.T., Sanchez, L., Esparza, T.J., and Brody, D.L. (2011). Distinct temporal and anatomical distributions of amyloid-beta and tau abnormalities following controlled cortical impact in transgenic mice. PloS One 6, e25475.
11. Uryu, K., Laurer, H., McIntosh, T., Pratico, D., Martinez, D., Leight, S., Lee, V.M., and Trojanowski, J.Q. (2002). Repetitive mild brain trauma accelerates Abeta deposition, lipid peroxidation, and cognitive impairment in a transgenic mouse model of Alzheimer amyloidosis. J. Neurosci. 22, 446–454.
12. Yoshiyama, Y., Uryu, K., Higuchi, M., Longhi, L., Hoover, R., Fujimoto, S., McIntosh, T., Lee, V.M., and Trojanowski, J.Q. (2005). Enhanced neurofibrillary tangle formation, cerebral atrophy, and cognitive deficits induced by repetitive mild brain injury in a transgenic tauopathy mouse model. J. Neurotrauma 22, 1134–1141.
13. McKee, A.C., Cairns, N.J., Dickson, D.W., Folkerth, R.D., Keene, C.D., Litvan, I., Perl, D.P., Stein, T.D., Vonsattel, J.P., Stewart, W., Tripodis, Y., Crary, J.F., Bieniek, K.F., Dams-O'Connor, K., Alvarez, V.E., Gordon, W.A.;TBI/CTE Group. (2016). The first NINDS/NIBIB consensus meeting to define neuropathological criteria for the diagnosis of chronic traumatic encephalopathy. Acta Neuropathol. 131, 75–86.
14. Mouzon, B., Chaytow, H., Crynen, G., Bachmeier, C., Stewart, J., Mullan, M., Stewart, W., and Crawford, F. (2012). Repetitive mild traumatic brain injury in a mouse model produces learning and memory deficits accompanied by histological changes. J. Neurotrauma 29, 2761–2773.
15. Ojo, J.O., Mouzon, B., Algamal, M., Leary, P., Lynch, C., Abdullah, L., Evans, J., Mullan, M., Bachmeier, C., Stewart, W., and Crawford, F. (2016). Chronic repetitive mild traumatic brain injury results in reduced cerebral blood flow, axonal injury, gliosis, and increased T-Tau and tau oligomers. J. Neuropathol. Exp. Neurol. 75, 636–655.
16. Kane, M.J., Angoa-Perez, M., Briggs, D.I., Viano, D.C., Kreipke, C.W., and Kuhn, D.M. (2012). A mouse model of human repetitive mild traumatic brain injury. J. Neurosci. Methods 203, 41–49.
17. Laurer, H.L., Bareyre, F.M., Lee, V.M., Trojanowski, J.Q., Longhi, L., Hoover, R., Saatman, K.E., Raghupathi, R., Hoshino, S., Grady, M.S., and McIntosh, T.K. (2001). Mild head injury increasing the brain's vulnerability to a second concussive impact. J. Neurosurg. 95, 859–870.
18. Meehan, W.P., 3rd, Zhang, J., Mannix, R., and Whalen, M.J. (2012). Increasing recovery time between injuries improves cognitive outcome after repetitive mild concussive brain injuries in mice. Neurosurgery 71, 885–891.
19. Shitaka, Y., Tran, H.T., Bennett, R.E., Sanchez, L., Levy, M.A., Dikranian, K., and Brody, D.L. (2011). Repetitive closed-skull traumatic brain injury in mice causes persistent multifocal axonal injury and microglial reactivity. J. Neuropathol. Exp. Neurol. 70, 551–567.
20. Winston, C.N., Noel, A., Neustadtl, A., Parsadanian, M., Barton, D.J., Chellappa, D., Wilkins, T.E., Alikhani, A.D., Zapple, D.N., Villapol, S., Planel, E., and Burns, M.P. (2016). Dendritic spine loss and chronic white matter inflammation in a mouse model of highly repetitive head trauma. Am. J. Pathol. 186, 552–567.
21. Ojo, J.O., Mouzon, B.C., and Crawford, F. (2016). Repetitive head trauma, chronic traumatic encephalopathy and tau: challenges in translating from mice to men. Exp. Neurol. 275 Pt 3, 389–404.
22. Ojo, J.O., Mouzon, B., Greenberg, M.B., Bachmeier, C., Mullan, M., and Crawford, F. (2013). Repetitive mild traumatic brain injury augments tau pathology and glial activation in aged hTau mice. J. Neuropathol. Exp. Neurol. 72, 137–151.
23. Petraglia, A.L., Plog, B.A., Dayawansa, S., Dashnaw, M.L., Czerniecka, K., Walker, C.T., Chen, M., Hyrien, O., Iliff, J.J., Deane, R., Huang, J.H., and Nedergaard, M. (2014). The pathophysiology underlying repetitive mild traumatic brain injury in a novel mouse model of chronic traumatic encephalopathy. Surg. Neurol. Int. 5, 184.
24. Andorfer, C., Kress, Y., Espinoza, M., de Silva, R., Tucker, K.L., Barde, Y.A., Duff, K., and Davies, P. (2003). Hyperphosphorylation and aggregation of tau in mice expressing normal human tau isoforms. J. Neurochem. 86, 582–590.
25. Duff, K., Knight, H., Refolo, L.M., Sanders, S., Yu, X., Picciano, M., Malester, B., Hutton, M., Adamson, J., Goedert, M., Burki, K., and Davies, P. (2000). Characterization of pathology in transgenic mice over-expressing human genomic and cDNA tau transgenes. Neurobiol. Dis. 7, 87–98.
26. Mouzon, B.C., Bachmeier, C., Ferro, A., Ojo, J.O., Crynen, G., Acker, C.M., Davies, P., Mullan, M., Stewart, W., and Crawford, F. (2014). Chronic neuropathological and neurobehavioral changes in a repetitive mild traumatic brain injury model. Ann. Neurol. 75, 241–254.

27. Mouzon, B.C., Bachmeier, C., Ojo, J.O., Acker, C.M., Ferguson, S., Paris, D., Ait-Ghezala, G., Crynen, G., Davies, P., Mullan, M., Stewart, W., and Crawford, F. (2018). Lifelong behavioral and neuropathological consequences of repetitive mild traumatic brain injury. Ann. Clin. Transl. Nerol. 5, 64–80.
28. Jicha, G.A., O'Donnell, A., Weaver, C., Angeletti, R., and Davies, P. (1999). Hierarchical phosphorylation of recombinant tau by the paired-helical filament-associated protein kinase is dependent on cyclic AMP-dependent protein kinase. J. Neurochem. 72, 214–224.
29. Ferguson, S.A., Mouzon, B.C., Lynch, C., Lungmus, C., Morin, A., Crynen, G., Carper, B., Bieler, G., Mufson, E.J., Stewart, W., Mullan, M., and Crawford, F. (2017). Negative impact of female sex on outcomes from repetitive mild traumatic brain injury in hTau mice is age dependent: a chronic effects of Neurotrauma Consortium Study. Front. Aging Neurosci. 9, 416.
30. Ferguson, S., Mouzon, B., Paris, D., Aponte, D., Abdullah, L., Stewart, W., Mullan, M., and Crawford, F. (2017). Acute or delayed treatment with anatabine improves spatial memory and reduces pathological sequelae at late time-points after repetitive mild traumatic brain injury. J. Neurotrauma 34, 1676–1691.
31. Hawkins, B.E., Krishnamurthy, S., Castillo-Carranza, D.L., Sengupta, U., Prough, D.S., Jackson, G.R., DeWitt, D.S., and Kayed, R. (2013). Rapid accumulation of endogenous tau oligomers in a rat model of traumatic brain injury: possible link between traumatic brain injury and sporadic tauopathies. J. Biol. Chem. 288, 17042–17050.
32. Schraen-Maschke, S., Sergeant, N., Dhaenens, C.M., Bombois, S., Deramecourt, V., Caillet-Boudin, M.L., Pasquier, F., Maurage, C.A., Sablonniere, B., Vanmechelen, E., and Buee, L. (2008). Tau as a biomarker of neurodegenerative diseases. Biomark. Med. 2, 363–384.
33. Lewis, J., McGowan, E., Rockwood, J., Melrose, H., Nacharaju, P., Van Slegtenhorst, M., Gwinn-Hardy, K., Paul Murphy, M., Baker, M., Yu, X., Duff, K., Hardy, J., Corral, A., Lin, W.L., Yen, S.H., Dickson, D.W., Davies, P., and Hutton, M. (2000). Neurofibrillary tangles, amyotrophy and progressive motor disturbance in mice expressing mutant (P301L) tau protein. Nat. Genet. 25, 402–405.
34. Yoshiyama, Y., Higuchi, M., Zhang, B., Huang, S.M., Iwata, N., Saido, T.C., Maeda, J., Suhara, T., Trojanowski, J.Q., and Lee, V.M. (2007). Synapse loss and microglial activation precede tangles in a P301S tauopathy mouse model. Neuron 53, 337–351.
35. Zhong, Q., Congdon, E.E., Nagaraja, H.N., and Kuret, J. (2012). Tau isoform composition influences rate and extent of filament formation. J. Biol. Chem. 287, 20711–20719.
36. Schneider, A., Biernat, J., von Bergen, M., Mandelkow, E., and Mandelkow, E.M. (1999). Phosphorylation that detaches tau protein from microtubules (Ser262, Ser214) also protects it against aggregation into Alzheimer paired helical filaments. Biochemistry 38, 3549–3558.
37. Arendt, T., Stieler, J., Strijkstra, A.M., Hut, R.A., Rudiger, J., Van der Zee, E.A., Harkany, T., Holzer, M., and Hartig, W. (2003). Reversible paired helical filament-like phosphorylation of tau is an adaptive process associated with neuronal plasticity in hibernating animals. J. Neurosci. 23, 6972–6981.
38. Arendt, T. and Bullmann, T. (2013). Neuronal plasticity in hibernation and the proposed role of the microtubule-associated protein tau as a ''master switch'' regulating synaptic gain in neuronal networks. Am. J. Physiol. Regul. Integr. Comp. Physiol. 305, R478–R489.
39. Dave, K.R., Christian, S.L., Perez-Pinzon, M.A., and Drew, K.L. (2012). Neuroprotection: lessons from hibernators. Comp. Biochem. Physiol B Biochem. Mol. Biol. 162, 1–9.
40. Planel, E., Richter, K.E., Nolan, C.E., Finley, J.E., Liu, L., Wen, Y., Krishnamurthy, P., Herman, M., Wang, L., Schachter, J.B., Nelson, R.B., Lau, L.F., and Duff, K.E. (2007). Anesthesia leads to tau hyperphosphorylation through inhibition of phosphatase activity by hypothermia. J.Neurosci. 27, 3090–3097.
41. Run, X., Liang, Z., Zhang, L., Iqbal, K., Grundke-Iqbal, I., and Gong, C.X. (2009). Anesthesia induces phosphorylation of tau. J. Alzheimers Dis. 16, 619–626.
42. Whittington, R.A., Bretteville, A., Dickler, M.F., and Planel, E. (2013). Anesthesia and tau pathology. Prog. Neuropsychopharmacol. Biol. Psychiatry 47, 147–155.
43. Statler, K.D., Alexander, H., Vagni, V., Dixon, C.E., Clark, R.S., Jenkins, L., and Kochanek, P.M. (2006). Comparison of seven anesthetic agents on outcome after experimental traumatic brain injury in adult, male rats. J. Neurotrauma 23, 97–108.
44. Corsellis, J.A., Bruton, C.J., and Freeman-Browne, D. (1973). The aftermath of boxing. Psychol. Med. 3, 270–303.
45. McKee, A.C., Cantu, R.C., Nowinski, C.J., Hedley-Whyte, E.T., Gavett, B.E., Budson, A.E., Santini, V.E., Lee, H.S., Kubilus, C.A., and Stern, R.A. (2009). Chronic traumatic encephalopathy in athletes: progressive tauopathy after repetitive head injury. J. Neuropathol. Exp. Neurol. 68, 709–735.

Address correspondence to:
Benoit Mouzon, PhD
Roskamp Institute
2040 Whitfield Avenue
Sarasota, FL 34243

E-mail: bmouzon@roskampinstitute.org